Circulation Regime-Dependent Nonlinear Interactions during Northern Hemisphere Winter

PHILIP S. BROWN, JR.*, ANTHONY R. HANSEN** AND JOSEPH P. PANDOLFO*

*The Center for the Environment and Man, Inc., West Hartford, CT 06117
**Meteorology Research Center, Control Data Corporation, Minneapolis, MN 55440

(Manuscript received 29 April 1985, in final form 27 September 1985)

ABSTRACT

Average statistics for periods of large positive 500 mb height anomalies are compared to statistics for all other situations using NMC data for the 15 Januaries from 1963 to 1977. The 500 mb heights and geostrophic streamfunctions are represented as surface spherical harmonics, and energy and enstrophy spectra along with nonlinear wave–wave interaction statistics are computed.

Differences in 500 mb geopotential height variance, kinetic energy and enstrophy spectra occur between large positive anomaly events and other days in the two-dimensional spectral index band from roughly $n = 6$ to $n = 9$, where n is the degree of the associated Legendre function. The same index band experiences a reversal of both the usual kinetic energy and enstrophy cascades during large positive anomaly events. That is, the $6 \leq n \leq 9$ band gains energy and enstrophy from wave–wave interactions during the anomaly events and loses energy and enstrophy by the same process at other times. The source of this energy and enstrophy is higher index (smaller two-dimensional scale) waves. The indication is that the Atlantic cases are more subject to this cascade reversal than are Pacific events.

Our results suggest that the smaller scale, transient eddies may play a regime-dependent role in interactions with atmospheric circulation modes on the scale of the persistent anomalies. When interacting with larger-scale features, the role of smaller-scale transients may not always be dissipative.

1. Introduction

Studies of the interaction between transient eddies and the climatological-mean stationary flow indicate that although the enstrophy budget of stationary waves in midlatitudes appears to be maintained in part by the transient eddies (Holopainen and Oort, 1981), the effect of transient eddy heat transports overwhelms the vorticity transports in a potential vorticity budget, giving an overall dissipative role to the transients when interacting with the time mean flow (Youngblut and Sasamori, 1980; Holopainen et al., 1982). Further study has revealed that the long period transients (periods of 10 to 90 days) make a stronger contribution to this dissipative effect than do synoptic-scale (2.5 to 6 day period) transients (Lau and Holopainen, 1984). Van den Dool (1983), on the other hand, infers a potentially large role for high frequency transients in forcing monthly mean *anomalies*.

Theoretical studies have indicated that the large-scale wave pattern can act to modulate synoptic-scale baroclinic activity (Fredrickson, 1979) and that synoptic-scale transients can play an important role in maintaining equilibrium states, or "weather regimes", in certain models (Reinhold and Pierrehumbert, 1982; Kallen, 1981, 1982). In the present study, we will use observational data to examine whether the interaction between different scales of motion in a spherical harmonic framework is dependent upon the circulation regime characterizing the large-scale pattern. We use the large positive height anomaly events identified by Charney et al. (1981) to stratify the data in the 15 Januaries from 1963 to 1977. Statistically significant differences in the energy and enstrophy spectra as well as in the nonlinear wave–wave interactions are found.

Baer (1972) suggested that the degree of the Legendre function in a spherical harmonic representation of the data is the appropriate index to use when studying atmospheric spectra. Observational studies of nonlinear exchanges using this two-dimensional index have been made by Chen and Wiin-Nielsen (1978), Lambert (1981), and Boer and Shepherd (1983). Mean cascading during winter as calculated by Chen and Wiin-Nielsen, for example, shows that for $n = 1$ to 7 and $n = 19$ to 31, kinetic energy is gained through nonlinear interaction, with this energy being supplied by the modes with $n = 8$ to 18. In the enstrophy budget, modes with $n = 1$ to 7 gain a very small amount of enstrophy while a large loss of enstrophy from the range $n = 8$ to 18 is balanced by gains of higher index modes. The physical explanation of the occurrence of these wave–wave interactions in the atmosphere is that the dissipation of kinetic energy and enstrophy takes place in different wavenumber bands from where these quantities are generated. In the present study, a dataset spanning a longer time period than those considered in earlier

studies is used and attention is focused on interactions near the low wavenumber end of the spectrum.

First, we illustrate the differences in the height variance, kinetic energy, and enstrophy spectra of the large positive anomaly events (LPAs) compared to more normal circulations. The changes occur primarily in the spectral index band from $n = 6$ to 9. Guided by these results, we explore systematic differences in the nonlinear cascading. We find an apparently regime-dependent role of the smaller scale transient eddies when interacting with the spectral band that distinguishes the LPAs.

2. Data

The basic data used in this study are 500 mb geopotential heights from the NMC final analyses. For each January day in the years 1963–77, daily values of the geostrophic stream function are computed. By using January data only, we hope to avoid any complications due to the seasonal cycle. We present results for the 500 mb surface only because these results may be considered representative of the vertical average in the energy and enstrophy budgets. (Qualitatively similar results were obtained using 300 mb data.)

To perform the required spherical harmonic analyses, data are required over the entire sphere. The NMC grid, however, extends only from 90°N to about 15°N. Data must be extrapolated to fill the region from 15°N to the equator about which a symmetry assumption can be made to account for the Southern Hemisphere. In order to generate the required data, Ellsaesser's (1966) technique has been adopted. To construct values in the north equatorial region, data lying within the NMC octagon are used to extrapolate southward along the meridians using a linear function of $\sin(2\phi)$ as an extrapolation profile (ϕ = latitude). Even symmetry of the geopotential height about the equator is then assumed.

The fictitious data, of course, affect the spectral coefficients. Nevertheless, we would not expect the introduction of such data to keep us from our main objective of identifying essential differences between spectra for different periods as long as the manufactured data are based on reasonable, though crude, physical assumptions. Comparison of our results obtained in this way to those of Boer and Shepherd (1983) in which global data were used reveals quite similar results. Therefore, we do not expect the treatment of the tropics in the present study to dramatically affect the results.

In order to define periods of large positive anomaly events, we have adopted the criterion of Charney et al. (1981). In their work, time–longitude cross sections of departures of 500 mb heights from their climatological mean values at 50°N were examined for the 15 winter seasons that include the January months selected for this study. A period was designated as a large positive anomaly event if at any point on the 50°N latitude circle a positive anomaly of 200 gpm or more persists for 7 days or more. Some subjectivity was introduced in determining the beginning and end of each event (Charney et al., 1981). Table 1 lists the periods considered to be LPAs. The letter A, P or B in this table indicates whether the largest amplitude ridge occurred over the Atlantic or Europe (A), the Pacific Basin (P), or whether comparable amplitude ridges occurred over both oceans (B). Events listed of less than 7 day duration spanned the beginning or ending of the month in question. Note that the existence of a large positive height anomaly doesn't necessarily imply that a greater height variance overall will exist at any particular location or for any particular wavenumber (e.g., see the discussion in Charney et al., 1981).

Of the 465 days included in our analysis, there were 154 LPA days and 311 "normal" days according to the criterion used. A comparison of the characteristics of blocking and nonblocking days determined from purely subjective review of individual twice-daily weather charts for the 15 months in question yielded generally similar results to those from the objectively chosen LPA cases. However, our purpose is to compare diagnostic statistics from time periods characterized by persistent circulation anomalies to statistics from time periods in which such features were lacking. The relationship of LPAs to blocking is outside the scope of the present study.

3. Analysis

We compute a streamfunction ψ from the geostrophic balance equation:

$$f\nabla^2\psi + \nabla f \cdot \nabla\psi = g\nabla^2 z \qquad (1)$$

where f is the Coriolis parameter, g the acceleration of gravity, and z the height of the constant pressure surface. For the nondivergent component of the flow, the kinetic energy (K) and enstrophy (E) can then be written as

TABLE 1. January days (1963–77) on which LPA events took place.

1	8–21 January 1963 (P)
2	22–29 January 1963 (B)
3	30–31 January 1963 (P)
4	1–6 January 1965 (P)
5	1 January 1966 (P)
6	5–14 January 1967 (A)
7	1–5 January 1968 (B)
8	6–31 January 1968 (A)
9	1–2 January 1969 (B)
10	3–14 January 1969 (P)
11	11–25 January 1970 (A)
12	7–13 January 1971 (B)
13	15–31 January 1971 (P)
14	3–9 January 1973 (A)
15	1–10 January 1974 (P)
16	27–31 January 1975 (P)
17	6–12 January 1977 (A)

$$K = \frac{1}{4\pi}\int_{-1}^{1}\int_{0}^{2\pi}\frac{1}{2}\nabla\psi\cdot\nabla\psi d\lambda d\mu$$

$$= \frac{1}{4\pi}\int_{-1}^{1}\int_{0}^{2\pi}-\frac{1}{2}\psi\zeta d\lambda d\mu \quad (2)$$

$$E = \frac{1}{4\pi}\int_{-1}^{1}\int_{0}^{2\pi}-\frac{1}{2}\zeta^2 d\lambda d\mu \quad (3)$$

where $\mu = \sin\phi$ and ϕ is latitude. Other notation is conventional.

On a sphere, any real-valued function such as ψ can be written formally as a series of surface spherical harmonics in the form

$$\psi(\lambda, \mu) = \sum_{m=0}^{\infty}\sum_{n=m}^{\infty}(A_n^m \cos m\lambda + B_n^m \sin m\lambda)P_n^m(\mu) \quad (4)$$

where $P_n^m(\mu)$ is the associated Legendre function. The series is uniformly convergent (hence term-by-term differentiable) provided that it has continuous second derivatives over the whole sphere (Hobson, 1931, p. 602). Using the orthogonality properties of the Legendre functions, the coefficients A_n^m and B_n^m can be obtained from

$$\begin{Bmatrix}A_n^m\\B_n^m\end{Bmatrix} = \frac{\delta_m}{2\pi}\int_{-1}^{1}\int_{0}^{2\pi}\psi(\lambda, \mu)\begin{Bmatrix}\cos m\lambda\\\sin m\lambda\end{Bmatrix}P_n^m(\mu)d\lambda d\mu \quad (5)$$

where $\delta_m = 1$ for $m = 0$, and $\delta_m = 2$ for $m \neq 0$.

Series differentiability is an important consideration since we are to examine spectra obtained by application of various differential operators to series representations of the streamfunction. In particular, since $\zeta = \nabla^2\psi$, differentiability of (4) allows us to express the vorticity as

$$\zeta(\lambda, \mu) = \sum_{m=0}^{\infty}\sum_{n=m}^{\infty}-\frac{n(n+1)}{a^2}(A_n^m \cos m\lambda + B_n^m \sin m\lambda)P_n^m(\mu) \quad (6)$$

where a is the earth's radius.

The kinetic energy and enstrophy can then be written in series form as

$$K = \sum_{n=0}^{\infty}K_n = \sum_{n=0}^{\infty}\sum_{m=0}^{n}\frac{n(n+1)}{2a^2}\delta_m[(A_n^m)^2 + (B_n^m)^2] \quad (7)$$

$$E = \sum_{n=0}^{\infty}E_n = \sum_{n=0}^{\infty}\sum_{m=0}^{n}\frac{n^2(n+1)^2}{2a^4}\delta_m[(A_n^m)^2 + (B_n^m)^2]. \quad (8)$$

Equations governing the complete spectral energy and enstrophy budgets of the atmosphere can be obtained by differentiating (2) and (3) with respect to time and substituting from the vorticity equation. The appropriate vorticity equation for the atmosphere includes generation and dissipation terms as well as terms representing the advection of relative and planetary vorticity. It isn't possible to reliably estimate the former two terms with the available data so we will focus attention on the barotropic terms we can compute. Therefore, we won't present complete budget statistics but will emphasize a particular aspect of the problem, namely barotropic, nonlinear effects. The nondivergent, adiabatic, frictionless form of the vorticity equation may be written as

$$\frac{\partial\zeta}{\partial t} = -J(\psi, \zeta) - \frac{2\Omega}{a^2}\frac{\partial\psi}{\partial\lambda}, \quad (9)$$

where J denotes the Jacobian

$$J(\psi, \zeta) = \frac{1}{a^2}\left(\frac{\partial\psi}{\partial\mu}\frac{\partial\zeta}{\partial\lambda} - \frac{\partial\psi}{\partial\lambda}\frac{\partial\zeta}{\partial\mu}\right). \quad (10)$$

We can obtain simplified spectral forms of the kinetic energy and enstrophy budget equations by differentiating (2) and (3) with respect to time and using (4), (6) and (9). In particular, the derivatives of K and E can be represented as functions of n as:

$$\frac{dK_n}{dt} = I_n = \sum_{m=0}^{n}I_n^m = \sum_{m=0}^{n}\frac{1}{2}\delta_m(A_n^m q_n^m + B_n^m r_n^m). \quad (11)$$

$$\frac{dE_n}{dt} = J_n = \sum_{m=0}^{n}J_n^m = \sum_{m=0}^{n}\frac{1}{2}\frac{n(n+1)}{a^2}\delta_m(A_n^m q_n^m + B_n^m r_n^m). \quad (12)$$

Here, q_n^m and r_n^m are the amplitudes of the cosine and sine components of the harmonic expansion of $J(\psi, \zeta)$. That is,

$$\begin{Bmatrix}q_n^m\\r_n^m\end{Bmatrix} = \frac{1}{4\pi}\int_{-1}^{1}\int_{0}^{2\pi}J(\psi, \zeta)\begin{Bmatrix}\cos m\lambda\\\sin m\lambda\end{Bmatrix}P_n^m(\mu)d\lambda d\mu; \quad (13)$$

I_n^m and J_n^m measure the rate of gain (loss) of kinetic energy and enstrophy respectively in component (n, m) that results from a corresponding rate of loss (gain) in the remainder of the spectrum. The change in total kinetic energy or enstrophy due to wave–wave interactions is zero. Computational considerations related to calculating these spectra and nonlinear transfers are discussed in the Appendix.

As noted earlier, for a less approximate form of the vorticity equation, (11) and (12) would also contain generation and dissipation terms. When averaging over a large ensemble of days, the tendency term in the energy or enstrophy budget will effectively be zero so the effects of the wave–wave interactions must be balanced by the effects of generation and dissipation for a given value of n.

In truncating (4) or (6), we wish to retain all terms that correspond to waves resolvable by the original data.

If it is assumed that four grid points are required to resolve a wave adequately, the limit of resolution of our data is near zonal wavenumber $m = 18$. With comparable data reliability in both latitude and longitude, the limit of resolution in latitude as measured by the one-dimensional index $n - m$ (the number of zeroes of $P_n^m(\mu)$ between the poles) is also 18. However, for the sake of easy comparison with earlier studies, we have employed triangular truncation at $n = m = 30$ in order to retain information on higher order analysis modes that are present (e.g., Chen and Wiin-Nielsen, 1978). The effect of differing truncations on the nonlinear interaction statistics is also discussed in the Appendix. The results converge for increasing truncation even though the values of I_n^m or J_n^m are, in general, a function of the truncation (see Appendix). The values of I_n or J_n appear to be insensitive to the truncation for $n \leqslant 14$.

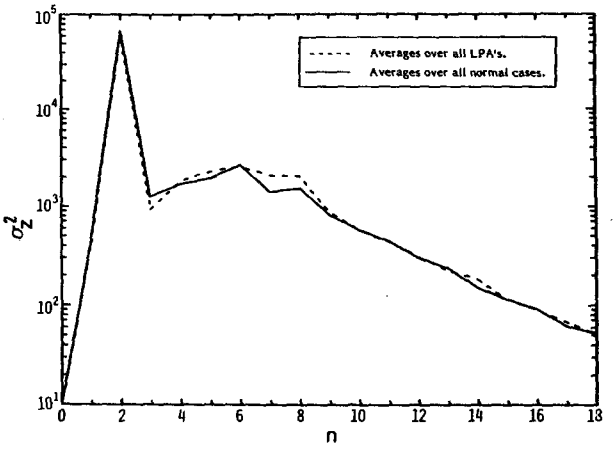

FIG. 1. Geopotential height variance σ_z^2 versus n for the 500 mb level.

4. Results

a. Spectra

Austin (1980) has shown that blocking situations are characterized by large amplitudes and normal phases for the zonal harmonic wavenumbers $m = 1$, 2, and 3. Pacific blocks in the mean exhibit greater amplitude for $m = 2$ and 3 while Atlantic blocks normally exhibit greater amplitude in wavenumbers 1 and 2.

To illustrate the characteristic signature of LPAs in the two-dimensional index n, let us first consider the spectrum of geopotential height variance,

$$\sigma_z^2 = \sum_{n=0}^{\infty} \left(\sum_{m=0}^{n} Z_n^m \right); \tag{14}$$

Z_n^m, the amplitude of spherical harmonic (n, m) for the 500 mb geopotential height, follows straightforwardly from the expansion of z in a series similar to (4). Figure 1 shows that the largest difference in σ_z^2 between LPAs and the balance of the data occurs at $n = 7$, 8 where LPAs have a greater variance. The LPAs also have slightly greater variance at $n = 5$ and slightly less at $n = 3$.

Examination of K and E spectra brings out an index band where differences between LPAs and the remainder of the sample are more systematic. The LPAs have greater kinetic energy in roughly the range $6 \leqslant n \leqslant 9$ (Fig. 2). The average increase in $\sum_{n=6}^{9} K_n$ is 30 percent for the LPAs compared to all other days. The statistical significance of this increase was tested with a two-sided t-test (Panofsky and Brier, 1958) assuming 5 days between independent samples of the 500 mb height. The differences in the K_n spectra are significant with greater than 99 percent confidence at $n = 7$, 95 percent at $n = 8$, and 90 percent at $n = 6$. The differences in K_n for the Atlantic cases alone are greatest at $n = 6$, 7 while the Pacific cases show particularly prominent differences at $n = 7$, 8 with smaller differences at $n = 6$ and 9 (not shown). Differences in the enstrophy spectrum (Fig. 3) closely follow those in K_n since $E_n = [n(n + 1)/a^2]K_n$. The stationary contribution to the K_n and E_n spectra was computed from the 15 January mean streamfunctions and is also displayed in Figs. 2 and 3. Note that the climatological mean stationary waves make significant contributions to the total K_n, for example, only for $n \leqslant 6$. For $n \geqslant 10$, the spectrum is dominated by transient waves (see also Boer and Shepherd, 1983).

Larger values of K_n or E_n imply greater dissipation since the dissipation is most likely related to the intensity of the wind in some way. Therefore, we might ask what mechanisms balance this dissipation and allow the noted increases in K_n and whether smaller scale waves act in a dissipative role.

b. Nonlinear exchange

We must keep in mind the inherent artificiality of describing atmospheric fluctuations in terms of the chosen (or any other) basis functions. The results for individual wavenumbers are often difficult to interpret. Therefore, it is traditional to form ensembles of wavenumbers with which to synthesize desired components of the flow (Saltzman and Fleisher, 1960; Wiin-Nielsen et al., 1963; Blackmon, 1976; Hansen and Chen, 1982). By analogy with the basic properties of Fourier transforms, these ensembles of wavenumbers allow specific features of the circulation to be synthesized (e.g.,, Hansen and Chen, 1982).

Blackmon (1976) has shown that geopotential height fluctuations with periods of 10–90 days are most important in the wavenumber regime, $7 \leqslant n \leqslant 12$. Lesser contributions to fluctuations of this period are made in the $1 \leqslant n \leqslant 6$ range. This is consistent with our finding that the major difference in the kinetic energy

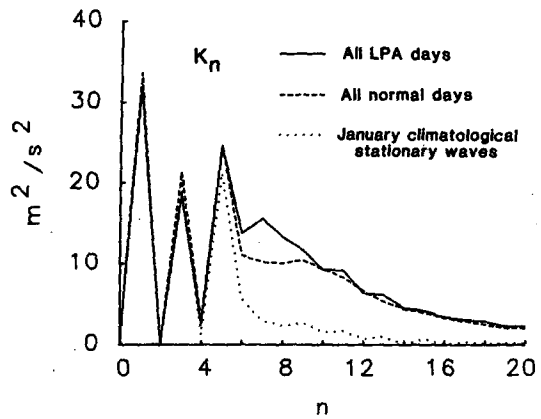

FIG. 2. Kinetic energy K_n versus n for the 500 mb level for LPA events (solid line); non-LPA events (dashed line) and for the 15 January climatological mean stationary waves (dotted line).

spectra between LPAs and the balance of our data occur in the range $6 \leqslant n \leqslant 9$.

The selection of the wavenumber ensembles we shall use presently was based on the differences in the spectra and was motivated as follows. First of all, harmonics with $1 \leqslant n \leqslant 5$ are grouped together because these modes represent the gross, mean features of the circulation and are very steady in time (Blackmon, 1976; Boer and Shepherd, 1983). In the present dataset, the content of K_n and E_n for $1 \leqslant n \leqslant 5$ is due almost entirely to the climatological mean waves (Fig. 2). In addition, there is virtually no difference in the mean K_n spectra, for example, between LPAs and the other situations for these modes (Fig. 2).

A second ensemble is formed from the harmonics with $6 \leqslant n \leqslant 9$. This grouping is due to the mean increase in the K and E content of this ensemble during LPA events. Note that this ensemble contains zonal wavenumbers from $m = 0$ through $m = 9$ and includes 18 different spherical harmonics. Thus, depending on the relative amplitudes and phases of the components in specific realizations, relatively localized features can be described. A third ensemble corresponding to smaller two-dimensional scale waves is formed from waves with $n \geqslant 10$. These ensembles provide a convenient way to visualize the results, but they are by no means unique. For example, based on differences in the cascading alone, ensembles for $1 \leqslant n \leqslant 3$ and $4 \leqslant n \leqslant 10$ could be justified.

The formation of wavenumber ensembles in the two-dimensional index is not directly analogous to the procedure in the one-dimensional index used, for example, by Hansen and Chen (1982). Each of our three chosen ensembles for the index n contains zonal harmonic wavenumbers of planetary scale (e.g., Blackmon, 1976). However, these waves have different latitudinal scales and therefore different two dimensional indices.

The results of the calculation of I_n and J_n are presented in Tables 2 and 3, respectively.

The gain in energy for the $1 \leqslant n \leqslant 5$ ensemble is reduced during LPA events. This change is entirely due to the change at $n = 3$ which is partially offset by the changes at $n = 4$ and 5. Differences in the enstrophy cascade for this ensemble are small. However, we can see that in the range of $6 \leqslant n \leqslant 9$, when all the positive anomaly cases are taken together, there is a reversal in the sign of the kinetic energy *and* enstrophy cascade compared to the balance of the sample. That is, during the positive anomaly events, waves with $6 \leqslant n \leqslant 9$ gain both kinetic energy and enstrophy from the other waves due to wave–wave interactions, whereas at other times, this ensemble loses a comparable amount of K_n and E_n due to the same mechanism. The source of this energy and enstrophy is the higher n waves, especially those for which $10 \leqslant n \leqslant 14$, a region of the spectrum dominated by transient eddies (e.g., Fig. 2 of Boer and Shepherd, 1983). The difference in the kinetic energy cascade between LPA and non-LPA days, ΔI_n, is illustrated in Fig. 4. The implication is that smaller two-dimensional scale transients are making positive contributions to both the energy and enstrophy budgets of the LPA pattern during these events. This is a somewhat remarkable result considering the global-scale treatment of the data used here. These results represent average interactions over the entire Northern Hemisphere.

When the LPA events are subdivided into Atlantic and Pacific cases, the reversal of the cascades for the $6 \leqslant n \leqslant 9$ regime is much more pronounced for the Atlantic cases. For the Pacific cases, the enstrophy cascade also reverses but the kinetic energy added to this band due to wave–wave interactions is small.

Using the same procedures used with the energy spectra, tests of the statistical significance of the differences in I_n indicate greater than 99 percent confidence in the differences at $n = 3$, $n = 8$ and $n = 13$. At $n = 3$, the difference is due to a much smaller rate of gain of K_3 due to nonlinear interactions for LPA events.

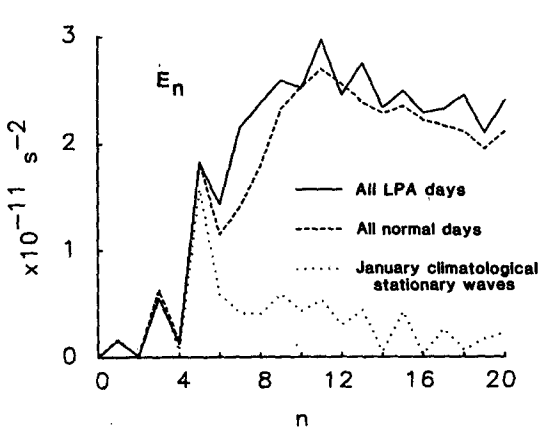

FIG. 3. Enstrophy E_n versus n for the 500 mb level for LPA events (solid line); non-LPA events (dashed line) and for the 15 January climatological mean stationary waves (dotted line).

TABLE 2. Time mean of I_n, the nonlinear kinetic energy exchange, for the various data samples. In this and subsequent tables, numbers to the right of the braces indicate sums over each wavenumber group. Units are 10^{-7} m^2 s^{-3}.

n	All non-LPA days		All LPA days		Atlantic LPA days		Pacific LPA days	
1	0		0		0		0	
2	−5		−2		−4		−1	
3	363	+550	213	+504	244	+473	201	+552
4	38		69		63		79	
5	154		224		170		273	
6	−12		31		91		−113	
7	−163		−164		−66		−198	
8	70	−143	224	+126	221	+282	261	−29
9	−38		35		36		21	
10	−71		−57		−99		8	
11	−120		−180		−220		−158	
12	−60		−93		−138		−56	
13	−34		−169		−182		−142	
14	−39		−92		−90		−97	
15	−77		−78		−93		−109	
16	−54		−35		−49		−26	
17	−64		−62		−53		−72	
18	−25		−38		−24		−45	
19	−8		0		4		9	
20	−17	−407	−36	−630	−40	−755	−35	−523
21	−9		11		17		12	
22	27		27		12		54	
23	15		−2		30		−38	
24	11		35		27		54	
25	22		38		35		32	
26	14		9		14		−10	
27	15		9		8		1	
28	22		35		31		35	
29	26		17		13		15	
30	19		31		42		36	

The difference at $n = 8$ represents a large increase in the rate of gain of K_8 due to nonlinear interactions and the difference at $n = 13$ represents a very large increase in the export of kinetic energy from $n = 13$ during LPA events. These statistically significant changes are consistent with the observed differences in the respective wavenumber ensembles in which these values of n occur (Table 2). These changes can easily be interpreted to indicate that on average during LPA events a greater amount of K_n (or E_n) is exported from the transient, high-index scales of motion (specifically $n = 13$) to the $n = 8$ region of the spectrum with less cascade toward very large scales, especially $n = 3$.

The large, significant changes in I_n at $n = 3$ and $n = 13$ are not accompanied by significant changes in K_n at these index values (although K_3 declines as one might expect if I_n is an important term in its budget), suggesting that nonlinear effects are compensated in some way. However, at $n = 8$ the significant increase in K_n is accompanied by a significant increase in the nonlinear contribution toward its maintenance. The increase in K_n at $n = 7$, on the other hand, requires an alternative, most likely baroclinic, energy source.

Our results by no means afford an explanation of the existence of the LPAs, but they do indicate the potential importance of cyclone-scale and small-scale transients in the maintenance of the LPA patterns, at least in a statistical sense. Saltzman (1959) first suggested that wave–wave interactions could act to maintain the quasi-permanent centers of action. More recently, Holopainen and Oort (1981) revived this idea and showed that transient eddies act to maintain the local energy and enstrophy balance of midlatitude, time-mean, standing waves as noted earlier. In the present context, wave–wave interactions act to diminish the K_n and E_n for modes in the $6 \leqslant n \leqslant 9$ bands during "normal" circulations. When the LPA subset (roughly ⅓ of the total sample) is examined, the noted reversal of this tendency appears.

We can also construct results for interactions in the one-dimensional index m, the zonal wavenumber, but these are not directly comparable to conventional studies of cascading in this one-dimensional index because the present results include interactions amongst all wavenumbers including the zonal mean wind components, $m = 0$. Conventional studies treat this wave–mean flow interaction separately (Saltzman, 1970). Nonetheless, if we compute the difference between

$$I_m = \sum_n I_n^m \quad \text{or} \quad J_m = \sum_n J_n^m \tag{15}$$

TABLE 3. Time mean of J_n, the nonlinear enstrophy exchange, for the various data samples, as in Table 2. Units are 10^{-18} s^{-3}.

n	All non-LPA days		All LPA days		Atlantic LPA days		Pacific LPA days	
1	0		0		0		0	
2	0		0		0		0	
3	11	24	6	26	7	23	6	30
4	2		3		3		4	
5	11		17		13		20	
6	−1		3		9		−12	
7	−23	−20	−23	28	−9	47	−27	12
8	12		40		39		46	
9	−8		8		8		5	
10	−19		−15		−27		2	
11	−39		−58		−71		−52	
12	−23		−36		−53		−21	
13	−15		−76		−82		−64	
14	−20		−47		−46		−50	
15	−45		−46		−55		−65	
16	−36		−24		−33		−18	
17	−48		−47		−40		−54	
18	−21		−32		−20		−38	
19	−8		0		3		9	
20	−18	−4	−37	−54	−42	−70	−37	−42
21	−10		13		19		14	
22	34		33		16		68	
23	20		−3		40		−51	
24	16		51		39		80	
25	35		61		57		52	
26	24		16		24		−1	
27	27		17		15		1	
28	44		69		63		71	
29	55		35		27		31	
30	43		72		96		81	

for the LPA events and the remainder of the dataset, differences similar to those found by Hansen and Sutera (1984) appear for the Atlantic cases (Table 4). In the mean for these cases, zonal wavenumbers 1–4 gain a large positive increment in K_m and E_m due to barotropic processes while the zonal mean flow ($m = 0$) receives less E and substantially less K during the Atlantic LPA events. For the Pacific cases, the zonal mean flow experiences even greater deficits from barotropic processes, but the enhanced upscale transfer from intermediate to large-scale waves does not appear.

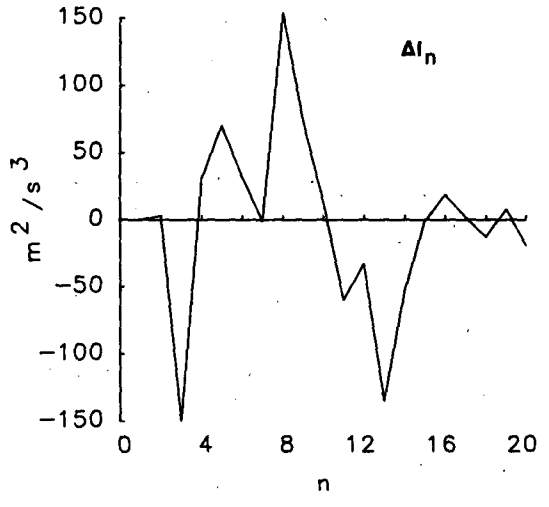

FIG. 4. The difference between the kinetic energy cascade for LPA events and all other times, ΔI_n, as a function of n. Results are only plotted for $n \leq 20$. For higher values of n, the differences are small (See Table 2). See text for interpretation of this figure.

In addition, results for a meridional index, $n - m$, can be constructed. We have arbitrarily grouped these waves in ensembles for $n - m = 1$ to 5, $n - m = 7$ to 15, and $n - m = 17$ to 29 for comparisons (Table 4 and Table 5). Note that the major differences between LPAs and the mean for other days in the sample occur at the low wavenumber end of the spectrum at $n - m = 5$. Modes with $n - m = 5$ roughly double their gain in kinetic energy, and their enstrophy cascade reverses. Similar characteristics appear when the LPA events are subdivided into Atlantic and Pacific cases (Table 5). Notice that the general characteristics of the nonlinear cascading in the meridional index are very similar to studies of cascading in the more conventional zonal index, m (Steinberg et al., 1971). In general, the differences in the one-dimensional indices at $1 \leq m \leq 4$ and $n - m = 5$ are consistent with the two-dimensional changes for $6 \leq n \leq 9$. The cascade of energy

TABLE 4. Differences, ΔI_j and ΔJ_j, in the nonlinear exchange of energy and enstrophy between the noted LPA events and the normal statistics for spectral index j. The results are listed for the various wave ensembles. Units for ΔI_j are 10^{-7} m^2 s^{-3} and for ΔJ_j are 10^{-18} s^{-3}.

	All LPA cases	Atlantic LPA cases	Pacific LPA cases	All LPA cases	Atlantic LPA cases	Pacific LPA cases
n		ΔI_n			ΔJ_n	
1–5	−46	−77	2	2	−1	6
6–9	269	425	114	48	67	32
10–30	−223	−348	−116	−50	−66	−38
m		ΔI_m			ΔJ_m	
0	−140	−74	−175	−24	−10	−35
1–4	46	158	−3	19	61	2
5–12	69	−120	160	−35	−99	2
13–30	25	36	18	40	48	31
$n-m$		ΔI_{nm}			ΔJ_{nm}	
1–5	325	237	318	79	31	91
7–15	−372	−297	−351	−136	−108	−122
17–29	47	60	33	57	−77	31

into the portion of the spectrum representing LPAs comes from eddies of smaller zonal and meridional scale.

5. Conclusion

Locally defined height anomalies leave statistically significant signals in hemispheric-scale circulation statistics. The major average differences in the kinetic energy and enstrophy spectra between the large, positive, persistent 500 mb height anomalies identified by Charney et al. (1981) and more normal circulations occur in the two-dimensional spectral index band $6 \leqslant n \leqslant 9$. The LPA events achieve both greater K_n and E_n on average in this region of the spectrum. Differences elsewhere are negligible. Statistically significant differences in the nonlinear cascading occur at $n = 3$, where less K and E are gained; at $n = 8$, where a tripling in the amount of K and E gained occurs; and at $n = 13$, where a very large increase in the amount of K and E lost occurs. Only the change in cascading at $n = 8$ is accompanied by a statistically significant change in K_n or E_n. These results imply that during LPA events, smaller two-dimensional scale transients add K and E to the wavenumbers characterizing the LPAs whereas during more zonal circulations wave–wave interactions act to dissipate this ensemble. Examination of differences in the cascading in 1 dimensional indices indicates that the transport of energy and enstrophy to the LPAs comes from eddies of both smaller zonal and

TABLE 5. Time mean of $I_{nm} = \sum_{n-m=\text{constant}} I_n^m$ and $J_{nm} = \sum_{n-m=\text{constant}} J_n^m$, the nonlinear exchanges of K and E in the meridional index, $n - m$. Wavenumber group sums are given to the right of braces. Units for I_{nm} are 10^{-7} m^2 s^{-3} and for J_{nm} are 10^{-18} s^{-3}.

	I_{nm}				J_{nm}			
$n-m$	Non-LPA days		LPA days		Non-LPA days		LPA days	
1	−68		−107		−16		−23	
3	116	340	143	665	−43	−75	−42	4
5	292		629		−16		69	
7	−194		−353		−37		−81	
9	−27		−125		−8		−43	
11	−108	−428	−182	−800	−40	−108	−70	−244
13	−57		−116		−18		−58	
15	−42		−24		−5		8	
17	−3		10		14		27	
19	17		25		38		45	
21	30		58		47		94	
23	23	58	40	135	39	183	67	240
25	18		1		38		1	
27	−1		−5		−3		−7	
29	4		6		10		13	

meridional extent. This suggests that the transients may play a regime dependent role in the dynamics of persistent circulation anomalies. The relative importance of these barotropic processes is an important question for further study. The study should be extended to determine the role of transient eddy heat transports in the dynamics of the anomalies. These results certainly do not imply that turbulent interactions alone are responsible for the existence of the anomalies. However, they do imply that the transients cannot be ignored or treated strictly as dissipative agents.

Acknowledgments. The authors names are listed in alphabetical order. This work was supported by the Division of Atmospheric Sciences of the National Science Foundation and under Grant ATM-8403372 at Control Data Corporation and under Grant ATM-8106034 at the Center for The Environment and Man, Inc. (CEM). One of us (ARH) was also supported by NASA under Grant NAS8-34903 while at Yale University. Computer support was provided by the National Center for Atmospheric Research (NCAR) which is sponsored by the National Science Foundation. The authors are grateful to Dr. Alfonso Sutera of CEM for numerous stimulating discussions, to Dr. Grant W. Branstator of NCAR for providing computer programs used for the harmonic analyses, to Prof. Michael Ghil of the Courant Institute for a helpful discussion in the planning stages of this project, and to Dr. G. D. Robinson of CEM for his guidance.

APPENDIX

Estimate of Truncation Error

In order to examine the energetics of LPAs and of normal flow, it is necessary to rely upon results that depend on derivatives of the basic variables in spite of inherent problems in evaluating such derivatives. The presence of higher order derivatives in the Jacobian form of (10), along with the nonlinearity of the expression, cause particular computational problems in evaluating the q_n^m, r_n^m (Eq. 13) that determine the wave–wave interaction coefficients. These derivatives may be calculated by finite differences or by term-by-term differentiation of series expansions. Finite differences introduce considerable truncation error, and so we have chosen the latter method of calculation. The termwise differentiation approach is not without problems either, due to the fact that the higher wavenumber, less reliable (i.e., more poorly resolved) components are amplified substantially in the differentiation process. Construction of the expansion for $\zeta (=\nabla^2\psi)$, for example, entails multiplication of ψ-coefficients by the factor $n(n+1)$ by virtue of the relation

$$\nabla^2\begin{Bmatrix}\cos m\lambda\\ \sin m\lambda\end{Bmatrix}P_n^m(\mu) = \frac{-1}{a^2}\, n(n+1)\begin{Bmatrix}\cos m\lambda\\ \sin m\lambda\end{Bmatrix}P_n^m(\mu). \tag{A-1}$$

It follows further that in the series for $\partial\zeta/\partial\mu$, the ψ-coefficients (A_n^m, B_n^m) are multiplied by factors that are $O(n^3)$. Derived expansions of this type are used to evaluate each of the for derivatives comprising the Jacobian.

When the expansions for the derivatives are used to form the product terms found in (10), interactions occur between waves of different index. In particular, high wavenumber harmonics interact to form lower-wavenumber harmonics in the resultant expansion for J. Due to this situation, the calculated components of J are found to vary even at the lower wavenumbers as

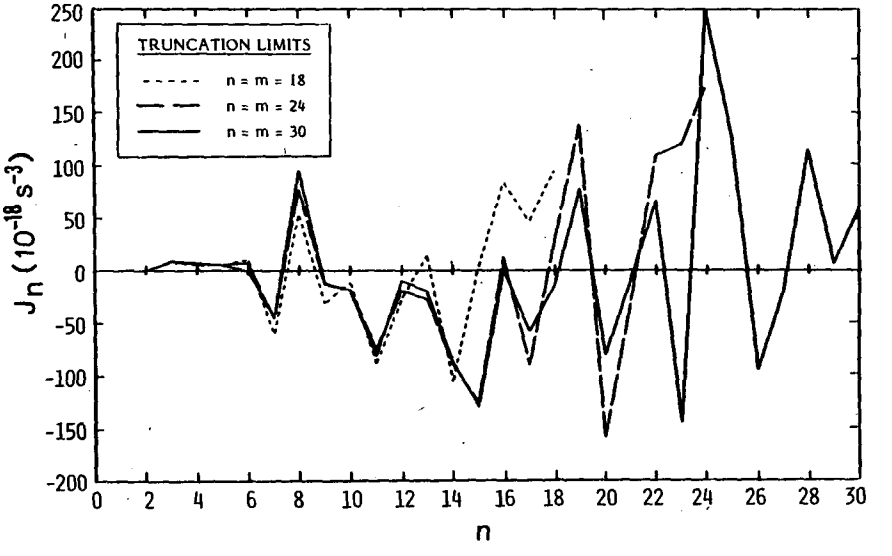

FIG. 5. J_n for the 24 LPA days in January 1963 for three different truncations.

the truncation limit is changed. Increasing the truncation limit of the individual series does not guarantee convergence of the results, however, since raising the limit serves to append components that are more poorly resolved and at the same time weighted more heavily. The high-wavenumber error in the differentiated series is distributed to the lower-wavenumber components as a result of the multiplications. Figure 5 shows the behavior of J_n versus n at 500 mb where the spectral coefficients have been averaged over the 24 LPA days of January 1963. The computations have been performed using triangular truncation with limits 18, 24 and 30. As the truncation is increased, the results for the 3 different truncations converge quite well for roughly $n \leqslant 14$. Comparing the truncations at $n = 24$ and $n = 30$ alone, the results appear to converge reasonably well for roughly $n \leqslant 18$.

REFERENCES

Austin, J. F., 1980: The blocking of middle latitude westerly winds by planetary waves. *Quart. J. Roy Meteor. Soc.*, **106,** 327–350.

Baer, F., 1972: An alternate scale representation of atmospheric energy spectra. *J. Atmos. Sci.*, **29,** 649–664.

Blackmon, M. L., 1976: A climatological spectral study of the 500 mb geopotential height of the Northern Hemisphere. *J. Atmos. Sci.*, **33,** 1607–1623.

Boer, G. J., and T. G. Shepherd, 1983: Large-scale two-dimensional turbulence in the atmosphere. *J. Atmos. Sci.*, **40,** 164–184.

Charney, J. G., J. Shukla and K. C. Mo, 1981: Comparison of a barotropic blocking theory with observation. *J. Atmos. Sci.*, **38,** 762–779.

Chen, T. C., and A. Wiin-Nielsen, 1978: On nonlinear cascades of atmospheric energy and enstrophy in a two-dimensional spectral index. *Tellus,* **30,** 313–322.

Ellsaesser, H. W., 1966: Expansion of hemispheric meteorological data in antisymmetric surface spherical harmonic (Laplace) series. *J. Appl. Meteor.*, **5,** 263–276.

Fredrickson, J. S., 1979: The effects of long planetary waves on the regions of cyclogenesis: Linear Theory. *J. Atmos. Sci.*, **36,** 195–204.

Hansen, A. R., and T. C. Chen, 1982: A spectral energetics analysis of atmospheric blocking. *Mon. Wea. Rev.*, **110,** 1146–1165.

——, and A. Sutera, 1984: A comparison of the spectral energy and enstrophy budgets of blocking versus nonblocking periods. *Tellus,* **36A,** 52–63.

Hobson, E. W., 1931: *The Theory of Spherical and Ellipsoidal Harmonics.* Cambridge University Press, 500 pp.

Holopainen, E. O., and A. H. Oort, 1981: On the role of large-scale transient eddies in the maintenance of the vorticity and enstrophy of the time-mean atmospheric flow. *J. Atmos. Sci.*, **38,** 270–280.

——, L. Rontu and N. C. Lau, 1982: The effect of large-scale transient eddies on the time-mean flow in the atmosphere. *J. Atmos. Sci.*, **39,** 1972–1984.

Kallen, E., 1981: The nonlinear effects of orographic and momentum forcing in a low-order, barotropic model. *J. Atmos. Sci.*, **39,** 2100–2163.

——, 1982: Bifurcation properties of quasi-geostrophic, barotropic models and their relation to atmosphere blocking. *Tellus,* **34,** 255–265.

Lambert, S. J., 1981: A diagnostic study of global energy and enstrophy fluxes and spectra. *Tellus,* **33,** 411–414.

Lau, N.-C., and E. O. Holopainen, 1984: Transient eddy forcing of the time-mean flow as identified by geopotential tendencies. *J. Atmos. Sci.*, **41,** 313–328.

Panofsky, H. A., and G. W. Brier, 1958: *Some Applications of Statistics to Meteorology.* The Pennsylvania State University Press, 224 pp.

Reinhold, B., and R. T. Pierrehumbert, 1982: Dynamics of weather regimes: Quasi-stationary waves and blocking. *Mon. Wea. Rev.*, **110,** 1105–1145.

Saltzman, B., 1959: On the maintenance of large-scale quasi-permanent disturbances in the atmosphere. *Tellus,* **11,** 427–431.

——, 1970: Large-scale atmospheric energetics in wavenumber domain. *Rev. Geophys. Space Phys.*, **8,** 289–302.

——, and A. Fleisher, 1960: The exchange of kinetic energy between larger scales of atmospheric motion. *Tellus,* **12,** 374–377.

Steinberg, H. L., A. Wiin-Nielsen and C. H. Yang, 1971: On nonlinear cascades in large-scale atmospheric flow. *J. Geophys. Res.*, **76,** 8629–8640.

Youngblut, C., and T. Sasamori, 1980: The nonlinear effects of transient and stationary eddies on the winter mean circulation. Part I: Diagnostic analysis. *J. Atmos. Sci.*, **37,** 1944–1957.

Van den Dool, H. M., 1983: A possible explanation of the observed persistence of monthly mean circulation anomalies. *Mon. Wea. Rev.*, **111,** 539–544.

Wiin-Nielsen, A., J. A. Brown and M. Drake, 1963: On atmospheric energy conversions between the zonal flow and the eddies. *Tellus,* **15,** 261–279.